Polish Journal of Medical Physics and Engineering
The Journal of Polish Society of Medical Physics
ISSN 1898-0309, doi: 10.2478/pjmpe-2026-0019

September 2026
Vol 32, Issue 3

Scientific Paper

Classification of Major Depressive Disorder Using EEG-Derived Brain, Ocular and Muscular Independent Components: A Preliminary Study

Seifeddine Babouri[1,ABCD*], Nabil Dib[1,BEF]

[1]*Department of Biomedical Engineering, Faculty of Technology, University of Abu Bekr Belkaid Tlemcen, Tlemcen, Algeria*
**Corresponding author: Babouri Seifeddine; seifeddine.babouri@univ-tlemcen.dz*

(received 01 March 2026; revised 23 May 2026; accepted 06 August 2026)

Abstract

Introduction: Electroencephalography (EEG) is widely employed for the automatic detection of Major Depressive Disorder (MDD), with most approaches focusing primarily on neural activity while discarding non-brain-derived components as artefacts. However, these non-neural sources may contain clinically relevant information, as they reflect the output of underlying neurophysiological processes.

Material and methods: In this study, we propose an EEG analysis framework that leverages components traditionally labeled as artefacts. Independent Component Analysis (ICA) was applied to a publicly available dataset comprising 34 subjects with depressive symptoms and 30 healthy controls to extract three categories of independent components (ICs): posterior brain ICs (Pb ICs), ocular ICs (Eye ICs), and electromyographic ICs (EMG ICs).

Features were extracted using the Wavelet Scattering Transform (WST), and classification was performed using a Long Short-Term Memory (LSTM) network. Model performance was evaluated across multiple values of the invariance scale (IS) parameter using a subject-level holdout split.

Results: The results indicate that classification performance was strongly dependent on the invariance scale (IS) parameter. Ocular ICs consistently provided higher discriminative performance across several configurations, whereas EMG ICs showed limited sensitivity. In contrast, posterior brain ICs did not exhibit meaningful discriminative performance, suggesting that reliable class-separating patterns could not be learned under the current experimental setup.

Conclusions: These findings suggest that non-neural EEG components, particularly ocular activity extracted via ICA, may contain useful information for MDD classification. However, given the use of a single subject-level split and the relatively small dataset size, the results should be considered preliminary. Further studies using more robust validation strategies and larger datasets are required to confirm the generalizability of this approach.

Keywords: LSTM, MDD diagnosis, ICA decomposition, Wavelet Scattering Transform, EEG sub-signals

Introduction

By definition, an individual is considered depressed once having persistent feelings of sadness and other depressive symptoms for at least three weeks consecutively. To prescreen for depression, the only clinically accepted methods are questionnaires to which the prospect will get to respond. The most commonly used tests are the DSM-V[1] and the Hamilton Rating Scale[2], as well as the Beck Depression Inventory (BDI)[3]. The problem with such tests lies in their subjectivity. Hence, the results will be closely related to the degree of collaboration of the subject. Furthermore, social pressure could dramatically reduce an individual's willingness to seek professional help promptly, thereby preventing early detection of the pathology. That is, looking for objective methods to diagnose depression is a necessity for overcoming the issues mentioned earlier.

An electroencephalogram (EEG) records the brain's electrical activity using a set of electrodes relative to a reference, according to standardized montages. The 10-20 and 10-10 systems are the most commonly used montages, with specific placements in different brain areas. The recorded EEG signal represents the electrical potential difference between each electrode and the reference, providing measurements with high temporal resolution. However, in most cases, these signals do not originate exclusively from the neural sources of interest. Instead, they are often contaminated by non-cerebral activities, commonly referred to as artifacts (e.g., ocular, muscular, and cardiac artifacts). These components are generally

© 2026 Authors This is an open access article licensed under the Creative Commons Attribution-NonCommercial-NoDerivs License (http://creativecommons.org/licenses/by-nc-nd/4.0/).

Authors' contribution: A – Research concept and design, B – Collection and/or assembly of data, C – Data analysis and interpretation, D – Writing the article, E – Critical revision of the article, F – Final approval of the article.

considered undesirable by researchers, and substantial efforts are therefore undertaken to detect, reduce, or remove them from the EEG data prior to analysis[4]. However, in some instances, signals of different origins cannot be easily separated with conventional filters, mainly when the frequency ranges overlap. That is, a technique based on blindly isolating different components of the signal is developed to visualize data from various sources; it's known as Independent Component Analysis (ICA). ICA is used in different areas, notably in speech-related studies, from which comes the cocktail party problem[5]. In neuroscience, ICA is typically used to remove undesirable components from the EEG signal, such as eye blinks and muscle movements. However, despite being labeled as parasites, these components could be valuable sources of information, and to the best of our knowledge, no study has discovered the potential of non-neural EEG components in the discrimination of brain disorders.

In recent years, Computer-Aided Diagnosis (CAD) techniques emerged to help enhance global health. In psychiatry, CADs can help address several situations by providing a reliable, non-subjective diagnosis. Hence, several studies employed electrophysiological signals as inputs to train Machine Learning (ML) models, yielding accurate discriminations between healthy and ill subjects. Due to the close relationship between these pathologies and different brain areas, EEGs have been the most studied electrophysiological signal for the prescreening of brain-related illnesses, including major depressive disorder (MDD).

Recent studies have extensively explored EEG-based machine learning frameworks for the automatic classification of MDD. Most existing approaches rely on time-frequency representations, functional connectivity measures, non-linear parameters, or mixed features, combined with either classical machine learning or deep learning (DL) models, often reporting classification accuracies exceeding 90%[6–12]. For instance, some studies have demonstrated that using stand-alone electrodes from specific scalp locations can yield competitive performance[7], whereas others have leveraged multi-electrode configurations or connectivity measures to capture interactions between distributed brain regions[8]. In addition, wavelet-based features have shown particularly strong performance due to their suitability for analyzing non-stationary electrophysiological signals[6,7,9]. Among these, the Wavelet Scattering Transform (WST) represents a modern extension of conventional wavelet analysis through a cascaded, convolutional architecture. As in the example of Sharma et al.[12], who employed scattering coefficients to train various ML classifiers for MDD discrimination on two datasets, namely GMC and MODMA, achieving accuracies of 99.95% and 99.3%, respectively.

Beyond EEG, several studies have explored alternative electrophysiological signals such as ECG[13–16], HRV[17,18], PPG[16,19], and respiratory signals (RSP)[16] in the context of depression, reporting encouraging classification performance. Additionally, Electrooculography (EOG) signals have shown strong discriminative power in applications such as ADHD detection[20], autism assessment[21], driver drowsiness monitoring[22], and alcohol intoxication analysis[23], with accuracies exceeding 80% in most cases. Moreover, a systematic review and meta-analysis[24] summarized the use of eye-tracking features in the context of MDD, identifying fixation count and saccade amplitude as the most extensively studied eye movement metrics. In parallel, several studies have investigated the usefulness of eye movements for depression discrimination. For instance, in Fang et al.,[25] eye-tracking measurements, combined with EEG and galvanic skin response (GSR), were integrated into a multimodal framework to train machine learning models, achieving encouraging classification performance. Zhu et al.[26] compared feature-based data fusion approaches with deep learning fusion classifiers using EEG and eye-tracking data. Their transformer-based framework, (MTNet), achieved an accuracy of 91.79%, with intermediate fusion yielding the best performance. Furthermore, Shen et al.[27] examined eye-tracking responses to emotional stimuli to assess attentional bias in depression. Their results indicated that individuals with depression exhibit longer gaze durations on negative images and slower attentional shifts toward other stimuli types. This approach achieved a maximum classification accuracy of 77.0%.

Similarly, cranial electromyogenic activity has been consistently linked to emotional states, mood disorders, and their treatment response[28–31]. EMG-based approaches either stand-alone or within multimodal frameworks have achieved high classification accuracies in emotion recognition tasks, often surpassing 90%[32–38], An exception is the study by Barigala et al.[35], which reported an accuracy of 70.6% using a Logistic Regression (LR) classifier. Early psychophysiological studies established the relevance of facial EMG in depression screening[39,40] and treatment response prediction[41], but its integration into modern machine learning pipelines remains limited.

Collectively, these findings indicate that eye and muscular signals may contain meaningful information related to affective and neurological states. These observations suggest that the systematic exclusion of non-neural EEG components may overlook potentially informative signals. Importantly, while ocular and EMG signals have been studied using dedicated sensors, their extraction directly from EEG recordings using ICA without additional hardware remains absent in the context of MDD classification.

Motivated by this gap, the present study investigates the discriminative potential of ICA-derived components from EEG recordings, including ocular, muscular, and posterior brain sources. The proposed framework combines ICA-based signal decomposition with feature extraction using the Wavelet Scattering Transform, followed by classification using a Long Short-Term Memory network (LSTM). Rather than focusing solely on achieving maximal classification performance, this work aims to explore the contribution of different signal sources and assess whether components traditionally considered artefactual can provide useful information for MDD discrimination. The study is therefore positioned as a preliminary investigation into the role of non-neural EEG components in machine learning-based depression detection.

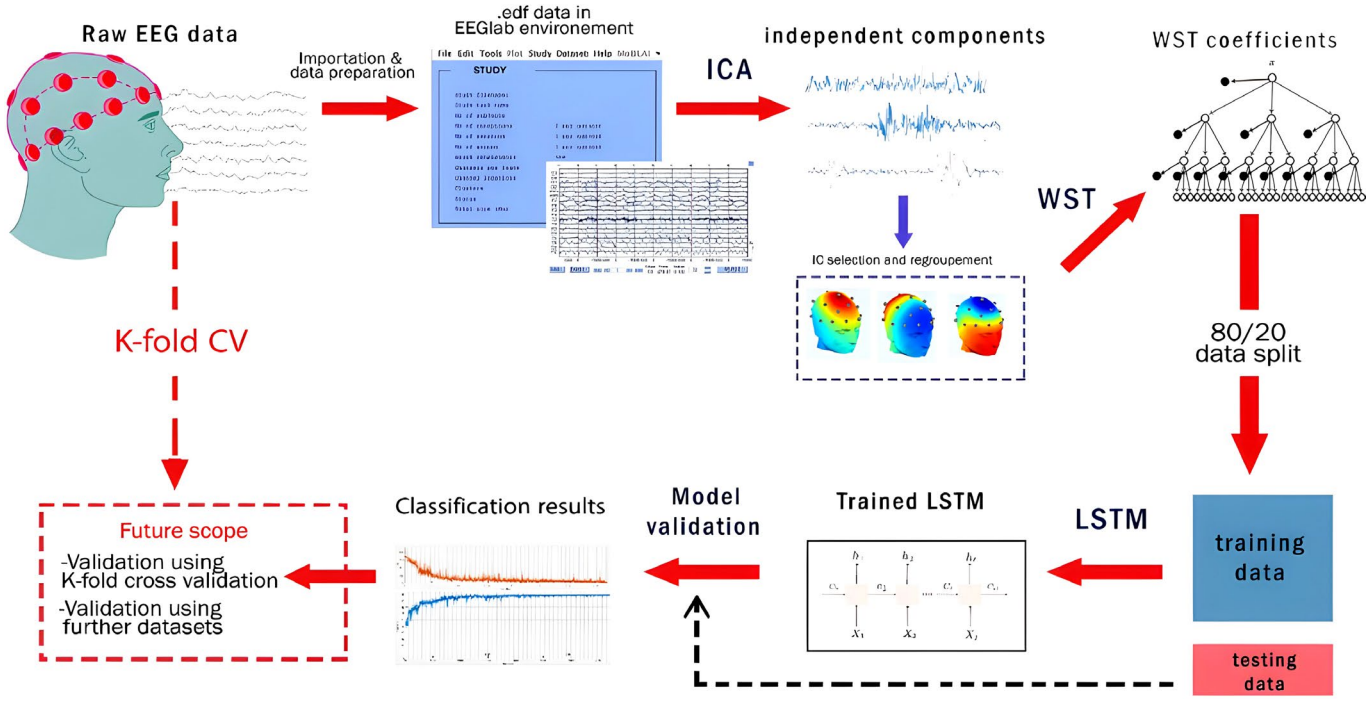


Figure 1. Study's pipeline

In this paper, ICA will be applied to EEG signals from depressive and healthy subjects to extract and compare three types of components: posterior brain components (Pb ICs), eye components (eye ICs), and muscle components (EEG ICs). **Figure 1** demonstrates the study's pipeline.

Materials and methods

Dataset

The experiment was conducted using a publicly available dataset introduced by Mumtaz[42], comprising 34 subjects diagnosed with major depressive disorder (MDD) (18 females; mean age = 40.33 ± 12.861 years) recruited from the University Hospital of Malaysia, in addition to 30 healthy control subjects (9 females; mean age = 38.227 ± 15.64 years). All participants voluntarily signed informed consent forms prior to enrollment, and the experimental protocol was approved by the hospital's ethics committee.

The diagnosis of depression was established according to the DSM-V criteria for unipolar depression[1], followed by additional clinical screening to exclude other psychological or physical disorders. EEG recordings of 5 minutes were acquired under both eyes-closed (EC) and eyes-open (EO) conditions using a 19-channel EEG cap based on the international 10–20 montage system with linked-ear (LE) referencing. However, only the EO recordings were retained in the present study in order to better preserve ocular dynamics and eye-related electrophysiological activity within the extracted independent components.

The EEG signals were collected from 19 electrodes distributed across frontal (Fp1, Fp2, F3, F4, F7, F8, Fz), central (C3, C4, Cz), parietal (P3, P4, Pz), temporal (T3, T4, T5, T6), and occipital (O1, O2) regions. After amplification using the BrainMaster acquisition system, the recordings were downsampled to 256 Hz. A 50 Hz notch filter was applied to suppress line noise interference, followed by high-pass and low-pass filtering with cutoff frequencies of 0.5 Hz and 70 Hz, respectively.

Wavelet Scattering Transform (WST)

The wavelet scattering transform is a relatively recent technique introduced by Mallat in 2012[43]. With a cascaded architecture, it operates similarly to a convolutional neural network (CNN). At each level of decomposition, a series of convolutions, complex modulus, and low-pass filtering is applied to the signal. WST offers more stability and robustness while minimizing computational cost, as it is time shift invariant and stable to deformation. One other advantage of the WST in comparison to the CNN model is the fixed weight of the wavelet filters; hence, no training is needed, making it less computationally intensive. The output of the WST is a rich representation of the input signal with interesting characteristics like energy conservation and invariance to translations and time shift. The signal x undergoes a series of iterated steps, where each iteration represents a deeper level of decomposition, considering the output of the level before as a new input. Firstly, the signal x is convolved with a mother wavelet ψ of center frequency λ, then a modulus operation is performed, similar to the pooling in the CNN. Furthermore, an averaging of the signal is made by convolving the output of the last two steps with a low-frequency father wavelet ϕ.

The 0_{th} order WST applied to the input signal x is by definition, the average of :

$$S_0 = x * \phi \qquad \text{Equation 1}$$

Wheraes the 1_{st} order WST of the signal x is defined as :

$$S_1 = |x * \psi_{\lambda_1}| * \phi \quad \text{Equation 2}$$

The 2_{nd} order WST is obtained by iterating the previously mentioned steps:

$$S_2 = || \left| x * \psi_{\lambda_1} \right| * \psi_{\lambda_2} || * \phi \quad \text{Equation 3}$$

LSTM classifier

A Recurrent Neural Network (RNN) is a deep learning architecture that employs hidden units to model complex temporal dependencies in sequential data. By maintaining cyclic connections, an RNN maps the current inputs together with information from previous time steps, enabling it to capture contextual information and improve prediction accuracy in classification tasks. However, standard RNNs suffer from limitations when processing long sequences, as they struggle to retain information from distant time steps due to the vanishing gradient problem. Long Short-Term Memory networks were introduced to overcome this limitation by incorporating a gating mechanism that regulates information flow and preserves relevant inputs over extended temporal intervals[44].

Model evaluation

In this study, the data were randomly split at a subject level, into two chunks: the first 80 was used for training, while the remaining 20 was held out for validation. Although some advanced techniques, such as k-fold cross-validation, would be more efficient for evaluating the model's generalization performance, the holdout method was used as a faster validation procedure. Values of Accuracy, Sensitivity, and Specificity were calculated to estimate the model's efficiency with concrete metrics:

$$\text{Accuracy} = \frac{TP + TN}{TP + TN + FP + FN} \quad \text{Equation 4}$$

$$\text{Sensitivity} = \frac{TP}{TP + FN} \quad \text{Equation 5}$$

$$\text{Specificity} = \frac{TN}{TN + FP} \quad \text{Equation 6}$$

Where TP represents the true positives or the number of patients correctly diagnosed with MDD, FN represents the false negatives or the MDD patients incorrectly labeled as healthy individuals, TN or true negatives representing the number of healthy individuals detected correctly, and FP or false positives representing the number of healthy individuals falsely diagnosed with MDD.

RunICA algorithm

EEGlab is a popular software known for its intuitive GUI and efficient processing of EEG time series. It was first presented by Delorme in 2004[45], and since then, it has undergone constant updates. RunICA is the implementation of the extended Infomax algorithm[46] in the EEGlab ecosystem. Infomax was first introduced by Bell and Sejnowski in 1995[47] and is considered one of the most widely adopted and influential ICA algorithms due to its computational efficiency and compatibility with neural data. Source separation is based on entropy maximization via gradient descent and a sigmoid nonlinearity to achieve statistical independence among components. The drawback of this version of the algorithm is that it is efficient only for separating mixtures with supergaussian distributions. To address this limitation, Lee et al.[46] introduced an extended version of the Infomax algorithm that preserves the simplicity of the first model while allowing it to separate a broader range of sources.

Unlike correlation-based blind source separation (BSS) techniques, such as principal component analysis (PCA), ICA exploits statistical dependencies to separate mixed sources most efficiently. From the algorithm's perspective, a real-world signal is a mixed set of linear and independent sources (i.e., sub-signals) that could be separated in an unsupervised manner. Mathematically, the ICA algorithm could be pretty complex and challenging to grasp; hence, the following lines present its framework in a simplified manner:

Assuming a signal $\mathbf{x}(t)$ is a mix of independent sources $\mathbf{s}(t)$ with $\mathbf{A}$ being the mixing matrix :

$$\mathbf{x}(t) = \mathbf{A}\mathbf{s}(t) \quad \text{Equation 7}$$

First the signal $\mathbf{x}(t)$ is centered :

$$\tilde{\mathbf{x}}(t) = \mathbf{x}(t) - \mathbb{E}\left[\mathbf{x}(t)\right] \quad \text{Equation 8}$$

Then, signal whitening (ie, sphering) is performed to decorrelate data sources:

$$\mathbf{z}(t) = \mathbf{V}\tilde{\mathbf{x}}(t), \quad \mathbb{E}\left[\mathbf{z}\mathbf{z}^{\top}\right] = \mathbf{I} \quad \text{Equation 9}$$

To estimate the unmixing matrix $\mathbf{W}$, the data is assumed to be both independent and non-Gaussian. ICA uses the non-Gaussianity measure $G(\cdot)$, to maximize the independence of the estimated sources $\mathbf{y}(t)$ in an iterative manner :

$$\max_{\mathbf{W}} \sum_{i=1}^{n} G(y_i) \quad \text{Equation 10}$$

The estimated sources will be determined as follow :

$$\hat{\mathbf{s}}(t) = \mathbf{y}(t) = \mathbf{W}\mathbf{x}(t) \quad \text{Equation 11}$$

EEG signal processing

Given that this study aims to compare different sources within EEG signals, minimal preprocessing was applied in order to preserve information relevant to the investigated components. However, signals exhibiting excessive noise were excluded from the analysis. The remaining EEG signals were first standardized, mean-centered, and normalized. A 50 Hz notch filter was then applied to remove residual line noise. No re-referencing was performed, and a high-pass filter with a cutoff frequency of 0.5 Hz was applied to ensure the removal of residual slow drifts not fully eliminated in the original preprocessing.

Independent Component Analysis (ICA) was performed using the RunICA algorithm to decompose EEG signals into

independent components. Topographic representations were then generated for each component. ICLabel[48] was used to automatically estimate the probability of each component belonging to predefined classes.

Based on both visual inspection and ICLabel outputs, three categories of components were selected for further analysis: ocular components (Eye ICs), muscular components (EMG ICs), and posterior brain components (Pb ICs). **Figure 2** illustrates representative ICA scalp maps associated with each category. Due to inter-subject variability, multiple spatial patterns may correspond to the same IC class, and component selection was therefore based on the prominence of the relevant source within each decomposition.

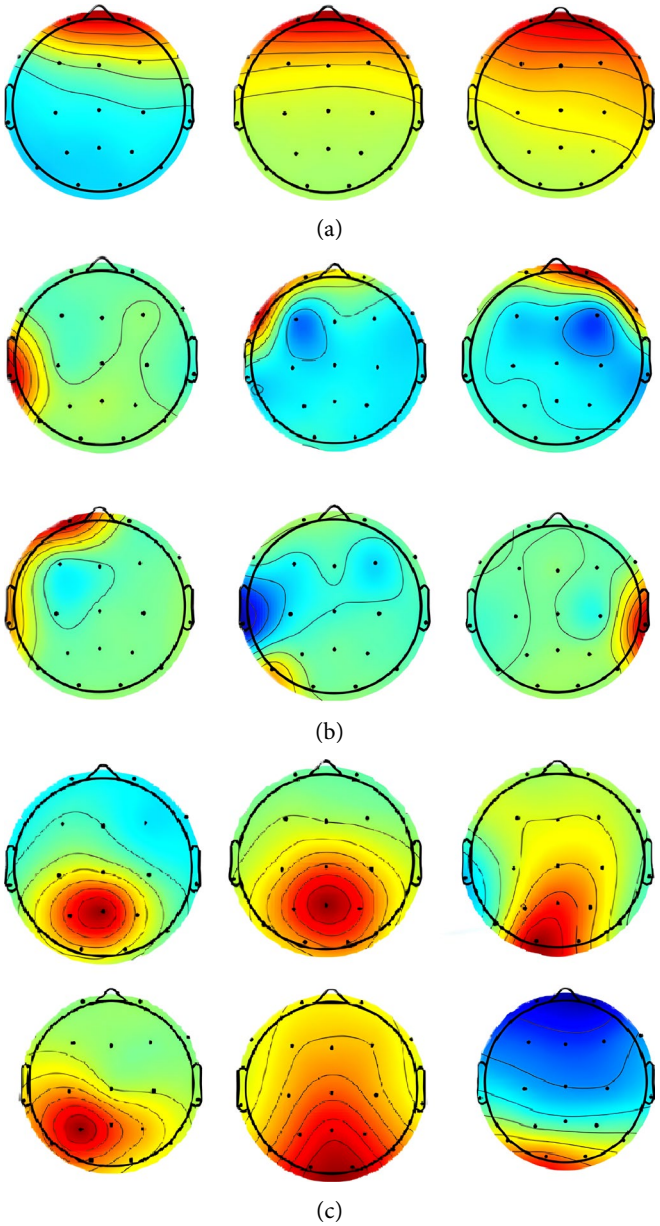


Figure 2. Representative examples of scalp maps associated with the different IC categories identified using manual inspection and ICLabel. Since ICA-derived components may exhibit inter-subject spatial variability, several representative topographical distributions are shown for each category. (a) Eye ICs. (b) EMG ICs. (c) Posterior brain ICs.

Not all participants necessarily exhibit all three component types, as ICA decomposition depends on the presence and strength of underlying sources in the EEG recordings. For instance, reduced movement during acquisition may result in weaker or absent muscular components. Afterwards, each IC category was organized into separate datasets, resulting in three independent data subsets. **Table 1** summarizes these datasets along with the corresponding number of healthy and depressive subjects.

Table1. Extracted datasets with the corresponding number of healthy and ill subjects.

Dataset	No. of H	No. of D
Eye ICs	28	29
EMG ICs	20	19
pB ICs	28	30

Abbreviations. No. of H: the number of healthy subjects. No. Of D: the number of depressed subjects.

Since EEGLAB does not directly provide standalone independent component time series as exportable signals, ICs were reconstructed by multiplying the ICA weight matrix, sphere matrix, and the original EEG signal, as described in **Algorithm 1.**

Algorithm 1. Computation of ICA Activations

Step1: Whitening:

$$X = EEG.icasphere \times EEG.data$$

Step2: ICA Activations:

$$EEG.icaact = EEG.icaweights \times X$$

Compact form:

$$EEG.icaact = (EEG.icaweights \times EEG.icasphere) \times EEG.data$$

Here, EEG.icaact represents the ICA activations (i.e., the estimated independent components), EEG.icaweights represents the ICA weights, EEG.icasphere denotes the sphering (whitening) matrix, and EEG.data corresponds to the recorded EEG signals.

WST decomposition

After reviewing the literature, only two levels of decomposition would be sufficient to extract the most relevant features, since 99% of the energy is found in the first and second levels[12,49,50,50]. Therefore, no more than three WST iterations were performed in this study. The quality factor Q represents the number of wavelets per octave in the wavelet filter bank. Different values of Q could be used at each decomposition level (L). For this study, values of Q1 = 8 and Q2 = 1 have been chosen for L1 and L2, respectively. These values are the default in most WST implementations. The invariance scale (IS) is another crucial hyperparameter to consider when using the WST. It defines the spacing between the wavelet output frequencies in the filter

banks, making it highly indicative of the dimensions of the WST output coefficients. For an output matrix of dimensions $M \times N$, increasing the invariance scale leads to a corresponding increase in N and a decrease in M, and vice versa. Given the central role of the IS in the study and its oversight in prior literature[12,49,50,50], different values of IS have been tested to determine the best-fitting configuration.

Classification with LSTM

The LSTM model consists of three layers with 100 neurons each and dropout layers with values of 0.2, 0.3, and 0.2, respectively. The dropout layers help prevent overfitting by randomly dropping neurons during training. This process allows the model to generalize, making it more robust and better able to withstand information scarcity. The three LSTM layers were followed by a fully connected layer then a softmax activation function with two output neurons was used to generate the final probability distribution for classification. It is noteworthy that a single sigmoid output unit is more commonly adopted for binary classification tasks; however, both formulations are mathematically equivalent in the binary case and lead to the same decision boundary.

The classification was performed using an Adam optimizer on a GPU, with a maximum of 128 epochs, a minimum batch size of 64, and a learning rate of 0.001. The configuration above was determined by empirically testing different combinations until the optimal settings were found. The holdout method with a subject-level 80/20 split was used to assess the training and testing procedures, ensuring no overlap between the two sets. The annotated data entries are first converted into a feature matrix before being fed to the LSTM model, and the test results are used in the evaluation process. **Figure 3** illustrates the architecture of the proposed model.

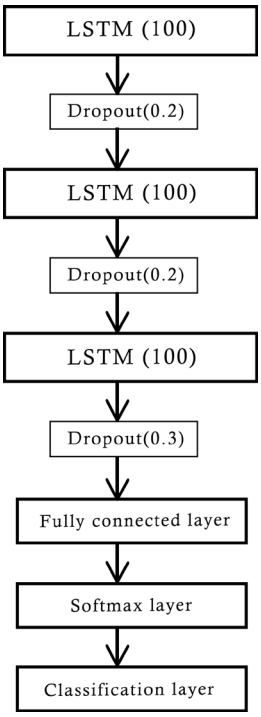


Figure 3. The architecture of the proposed model

Results

Table 1 summarizes the number of subjects contributing to each IC category. The results indicate that posterior brain component and ocular components are present in the majority of EEG recordings, whereas EMG-related components are less consistently observed across subjects. This distribution is further illustrated in **Figure 4.**

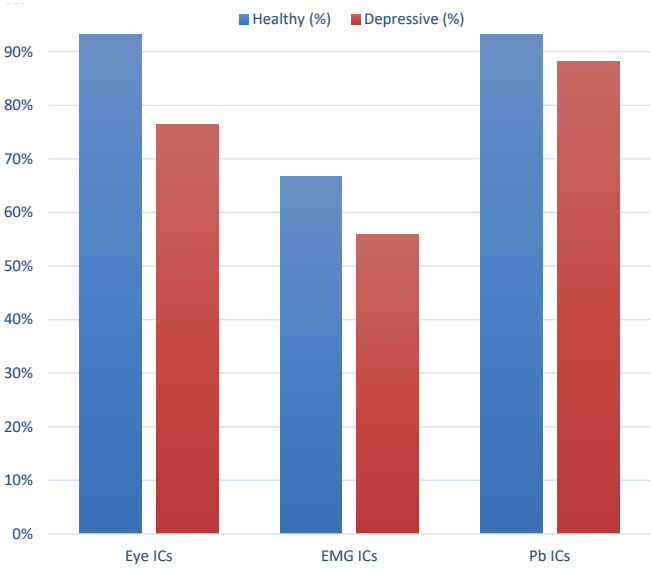


Figure 4. The frequency of the three extracted ICs from the dataset

Table 2 reports the optimal classification performance obtained using Eye and EMG IC categories and their corresponding confidence intervals, evaluated on a subject-level holdout test set. **Tables 3 and 4** present detailed classification results for Eye ICs and EMG ICs, respectively, across different values of the invariance scale parameter, along with the corresponding feature dimensionality. The results demonstrate a strong dependence of classification performance on the IS parameter, which influences both the temporal resolution and dimensionality of the WST features. Rather than identifying a single optimal configuration, the variability across IS values is considered an important observation of this study. It is important to note that although segmentation and WST-based processing produce a large number of training samples, these samples are derived from a limited number of subjects and therefore do not constitute statistically independent observations.

Table 2. Result of testing different IS values with the eye components.

IS value	Acc (%)	Sen (%)	Spec (%)	TMr	TMl	tMr	tMl
10	86.32	95.99	74.80	6686	204	1652	204
15	**98.32**	**98.90**	**97.61**	**3352**	**261**	**831**	**261**
20	88.92	96.46	79.89	3348	265	835	265
25	81.71	83.48	79.58	1684	328	421	328

Abreviations. Acc: accuracy. Sen: sensitivity. Spec: specificity. TMr: number of training matrix rows. TMl: number of training matrix lines. tMr: number of testing matrix rows. tMl: number of testing matrix lines.

Table 3. Result of testing different IS values with the EMG components.

IS value	Acc (%)	Sen (%)	Spec (%)	TMr	TMl	tMr	tMl
10	**71.24**	**45.14**	**97.21**	**4642**	**204**	**1217**	**204**
15	68.54	56.33	80.59	2336	261	604	661
20	70.83	93.43	50.33	2364	265	576	265
25	65.25	66.01	64.47	1174	328	305	328

Abreviations. Acc: accuracy. Sen: sensitivity. Spec: specificity. TMr: number of training matrix rows. TMl: number of training matrix lines. tMr: number of testing matrix rows. tMl: number of testing matrix lines.

Table 4. Maximum values of performance metrics for Different IC Types

IC Type	Accuracy(%)	Sensitivity(%)	Specificity(%)
Eye ICs	**98.32**	**98.9**	**97.61**
EMG ICs	71.24	45.14	97.21
pB ICs	45.32	1	0

To further assess the reliability of the best-performing configurations identified in **Tables 3 and 4**, 95% confidence intervals (CI) were computed using subject-level bootstrap resampling for the optimal IS value of each IC category. For Eye ICs, the results indicate high and stable performance with narrow confidence intervals: accuracy (97.47–99.04%), sensitivity (97.78–99.78%), and specificity (95.99–99.02%). For EMG ICs, lower and more variable performance was observed, reflected in wider confidence intervals: accuracy (68.69–73.79%), sensitivity (41.34–49.19%), and specificity (95.93–98.43%).

Figure 5 presents the test-set confusion matrices for the three IC categories, illustrating distinct classification behaviors across feature types. EMG ICs show higher misclassification rates, whereas Eye ICs demonstrate more balanced class separation. Posterior brain ICs exhibit near chance-level classification performance. **Figure 6** illustrates the evolution of training loss and training accuracy curves during model optimization. These curves reflect learning dynamics on the training data. For EMG ICs, a divergence between training and validation curves suggests potential overfitting, whereas Eye ICs show more coherent learning behavior.

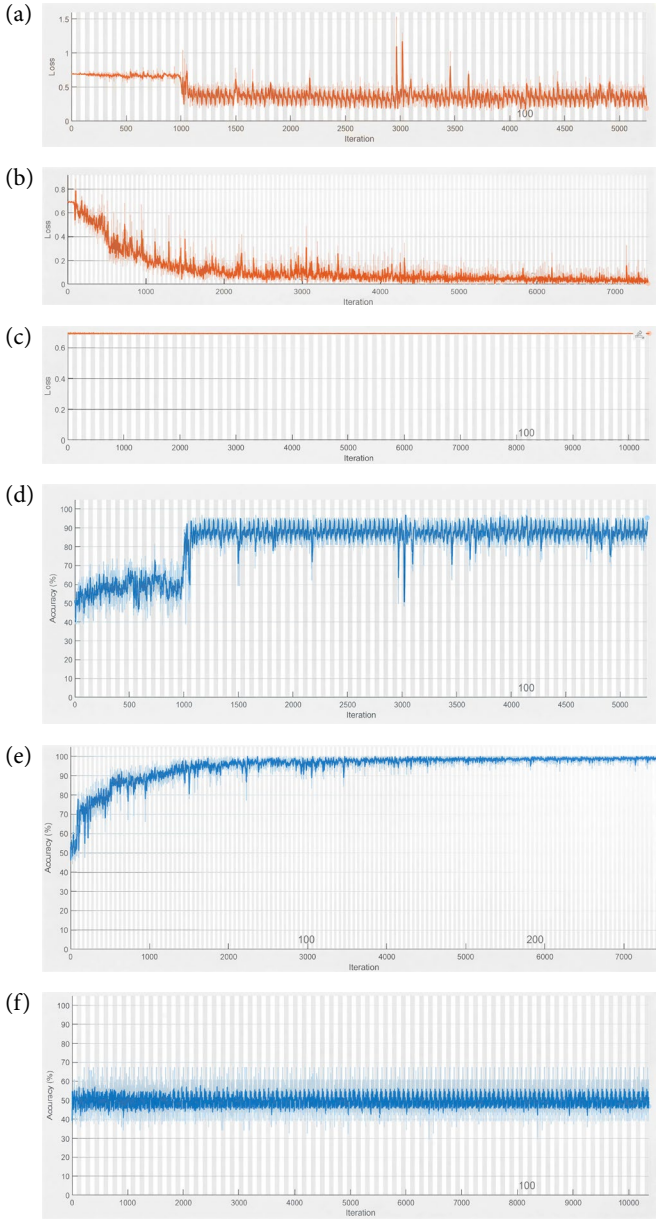
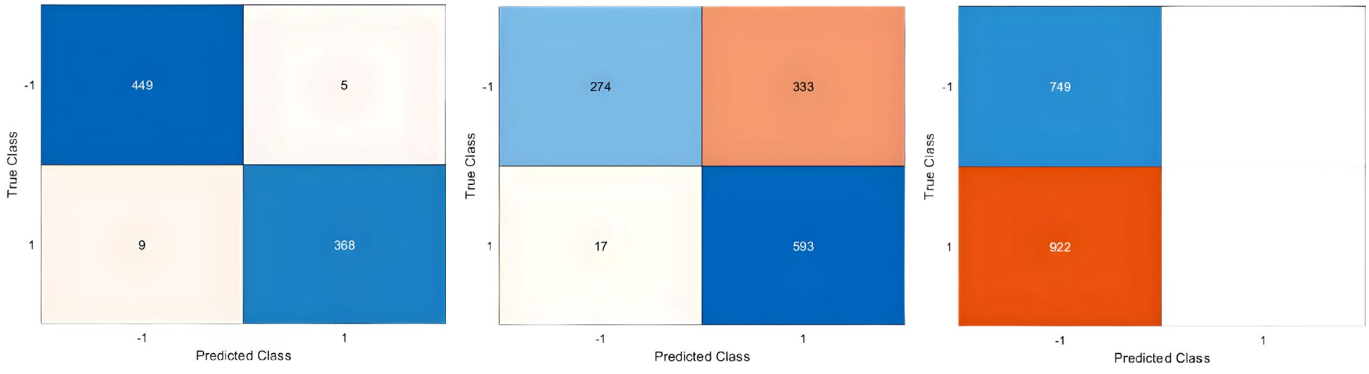


Figure 6. Evolution of the training loss and training accuracy curves for the three experiments. (a) Training loss curve of the eye ICs LSTM model. (b) Training loss curve of the EMG ICs LSTM model. (c) Training loss curve of the Pb ICs LSTM model. (d) Training accuracy curve of the eye ICs LSTM model. (e) Training accuracy curve of the EMG ICs LSTM model. (f) Training accuracy curve of the Pb ICs LSTM model.



(a) (b) (c)

Figure 5. Confusion matrices obtained on the holdout test set for the three classification experiments using different categories of independent components (ICs). (a) Eye ICs confusion matrix. (b) EMG ICs confusion matrix. (c) Posterior brain ICs confusion matrix.

Discussion

Eye ICs

Electrooculography measures ocular activity by modeling the eye as an electrical dipole, whereby eye movements and blinks generate measurable electrical potentials recorded by electrodes placed near the eyes. The morphology of the extracted eye-independent components closely resembles that of classical EOG signals as shown in **Figure 7**. In EEG recordings, frontal electrodes such as FP1 and FP2 are particularly sensitive to ocular activity due to volume conduction effects through the scalp[51]. Eye movement artifacts mainly result from changes in dipole orientation, whereas blinking artifacts are caused by corneal-eyelid contact and typically appear as large-amplitude transients in EEG recordings.

In conventional EEG preprocessing pipelines, such components are systematically removed[6–8,12]. However, the present results suggest that these non-neural components may contain discriminative information relevant to MDD classification**.** This observation is consistent with existing literature reporting systematic differences in eye movement behavior between depressive and non-depressive subjects, including alterations in saccadic dynamics and blink patterns[52,53]. Therefore, the contribution of this work is not the introduction of eye-related signals in depression studies per se, but rather the demonstration that ocular activity can be extracted directly from standard EEG recordings via ICA and exploited for classification without dedicated eye-measurement hardware**.**

From a modeling perspective, the use of temporal architectures such as LSTM may facilitate the capture of subtle temporal dynamics in ocular activity. Furthermore, eye movements are closely linked to affective and cognitive processes, and their modulation in mood disorders has been widely documented[32,33,54]. From a neurophysiological standpoint, oculomotor behavior is controlled by distributed cortical and subcortical networks, including the frontal eye fields, basal ganglia, brainstem, and cerebellum[55–57]. Consequently, Eye ICs may indirectly reflect alterations in these networks associated with MDD[52,53].

Finally, analysis of the model's learning behavior in **Figures 5a and 5d** revealed a gradual increase in training accuracy, with a steep rise starting from approximately 1000 iterations with a demonstration of a slight underfitting. However, it is important to emphasize that the reported performance should be interpreted with caution. Given the reliance on a single subject-level split and the observed sensitivity to hyperparameter selection (IS), these findings should be considered preliminary and require validation using more robust evaluation frameworks.

EMG ICs

The results obtained using EMG ICs show limited discriminative performance**,** particularly reflected by low sensitivity values. This suggests that, under the current experimental setup, muscular components alone are insufficient for reliable MDD classification. However, this does not necessarily imply that EMG-related activity is irrelevant. The observed performance may be influenced by several methodological factors. For instance, standard EEG acquisition and preprocessing are not optimized for capturing high-frequency muscular activity, potentially leading to partial loss of relevant information[58].

In contrast, dedicated facial EMG studies typically target specific muscle groups such as the corrugator supercilii or zygomaticus major, which are strongly associated with emotional expression[32–36]. The activation of these muscular groups reflect neural processes through their direct connection with the central nervous system[59] and may encode affective information even in the absence of overt facial expressions[60]. Therefore, the EMG ICs extracted in this study likely represent a coarse ap-

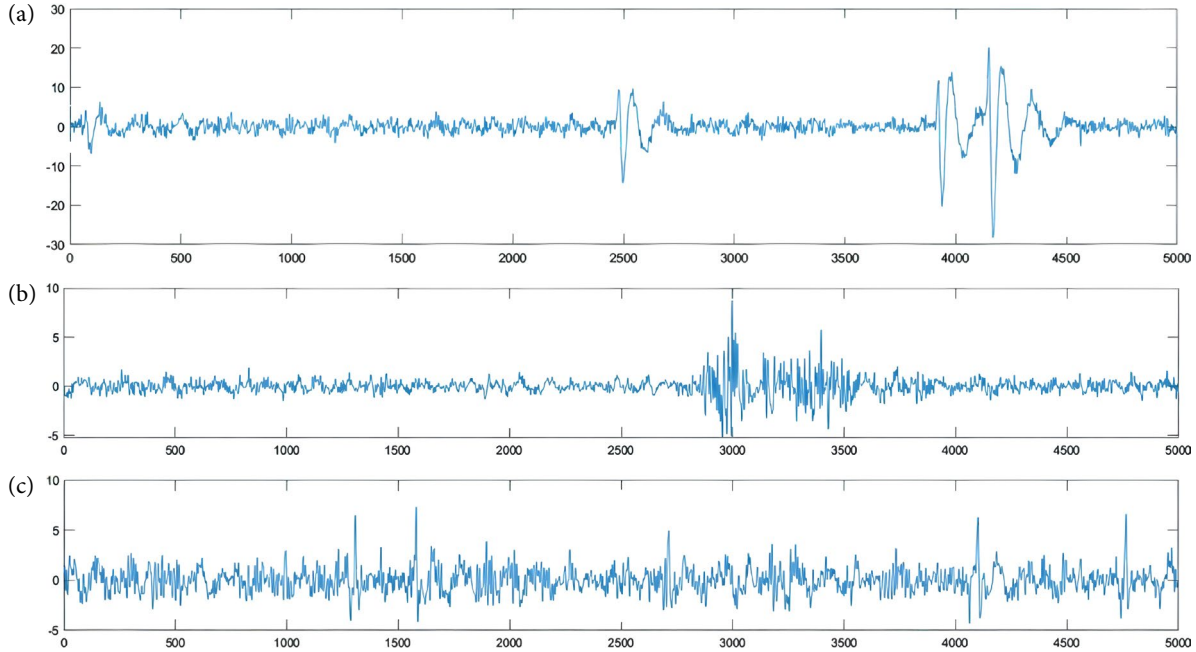


Figure 7. Plots of raw independent components. (a) raw eye sub-signal. (b) raw EMG sub-signal. (c) raw posterior brain sub-signal.

proximation of muscular activity and may not capture the full extent of emotion-related features. Additionally, the learning curves **(Figures 5b and 5e)** indicate overfitting, further limiting the reliability of the obtained results. Overall, EMG-based classification within this framework appears **limited and inconclusive,** and would likely require dedicated acquisition protocols and improved feature extraction strategies.

Posterior brain ICs

The study was initially designed to compare two non-neural sources with a category of brain components in order to enrich the research context. However, the classification results obtained using posterior brain ICs revealed near chance-level performance, with the model collapsing toward prediction of a single class. This suggests that meaningful discriminative patterns could not be reliably learned from these features under the current experimental conditions.

Although this outcome may appear counterintuitive, several factors may explain these results. First, ICA decomposition with a limited number of electrodes (19 channels) may not provide sufficiently reliable separation of neural sources, particularly when attempting to isolate specific cortical regions. Second, brain signals are inherently more complex, variable, and less stereotyped than ocular or muscular activity, making them more challenging to model using limited datasets. While posterior alpha activity has been associated with depression in prior studies, extracting stable and discriminative representations from such signals remains difficult.

This analysis focused on the posterior part of the brain, specifically its alpha activity. Posterior alpha rhythms have been extensively investigated in the literature and are known to play a central role in attention[61], prestimulus processin[62], and sensory inhibition[63]. Other studies have also highlighted their close relationship with depression, reporting reduced posterior alpha activity in depressive subjects compared to healthy controls[64,65].

The present findings suggest that, within this framework, posterior ICs do not provide sufficiently robust features for reliable classification. Rather than reflecting a modest reduction in performance, these results indicate limited separability between classes under the current experimental setup. As illustrated by the confusion matrix in **Figure 5c** and the learning curves **Figures 6c and 6f**, the model was unable to extract discriminative information sufficient for effective class separation. The obtained results suggest that the classifier converged toward a biased prediction strategy while minimizing the loss function under constrained learning conditions. Although alternative strategies such as threshold tuning could potentially enhance sensitivity, maintaining identical evaluation conditions across the three data types allows for a more consistent comparative analysis.

Comparison with existing studies on the Mumtaz dataset

Several studies using the Mumtaz dataset have reported high classification performance using conventional EEG-derived features, including spectral, connectivity-based, entropy-based, and deep learning approaches [6–12]. In contrast, the present work does not rely on cleaned multichannel EEG activity, but instead investigates ICA-derived non-neural components extracted directly from standard EEG recordings. Consequently, direct comparison of classification performance should be interpreted cautiously, as the objective of the present study was not primarily performance optimization, but rather the evaluation of the discriminative potential of different ICA-derived sub-signals. Nevertheless, the acceptable performance observed for eye ICs suggests that ocular-related activity embedded within EEG recordings may contain physiologically relevant information for MDD discrimination.

Conclusion

In this paper, the relevance of independent components extracted from EEG signals was investigated for the automatic classification of major depressive disorder. The findings highlight an alternative perspective on the exploitation of non-neural EEG components, which may reflect indirect manifestations of underlying neurophysiological processes. The primary objective was to assess whether these sub-signals contain discriminative information or should instead be systematically excluded during EEG preprocessing. To this end, raw EEG recordings were analyzed with minimal preprocessing prior to ICA decomposition using EEGLAB.

Among the investigated component categories, eye ICs demonstrated the highest discriminative potential. These components, which reflect activity associated with the oculomotor system and eye movements, appeared to carry information related to the subject's internal affective state. This observation challenges the conventional characterization of ocular EEG components as mere "eye-blinking artifacts" and suggests that they may constitute informative physiological signals in the context of MDD analysis. Given that most EEG-based depression studies primarily focus on neural activity following artifact rejection, the present findings support further investigation of ICA-derived non-neural components within psychiatric EEG analysis pipelines.

Conversely, the results obtained using EMG ICs remained limited and inconclusive, likely due in part to the attenuation of high-frequency muscular activity during acquisition and preprocessing. Similarly, posterior brain ICs exhibited near chance classification behavior, suggesting that the isolated components did not preserve sufficiently discriminative information under the current framework. This may reflect the intrinsic difficulty of reliably separating localized neural sources from low-density EEG recordings using ICA.

Overall, the present work should be regarded as a preliminary study exploring the potential relevance of ICA-derived non-neural EEG components for MDD discrimination. Although the reported findings require validation on larger datasets and under more rigorous subject-level cross-validation strategies, they suggest that systematically excluding non-encephalic EEG components may lead to the loss of physiologically relevant information [66].

Limitations

This study should be regarded as a preliminary exploration of the discriminative potential of ICA-derived EEG sub-signals for major depressive disorder classification. Several limitations should therefore be considered when interpreting the reported findings. First, model evaluation relied on a single subject-level holdout split, which may not fully capture performance variability across different train-test partitions. More rigorous validation strategies, such as repeated subject-level cross-validation or nested cross-validation, should be employed in future work to obtain more robust generalization estimates. In addition, the investigated dataset remains relatively limited in size, particularly after separating the recordings into different IC categories, which restricts the statistical reliability of deep learning-based evaluation.

Second, the study focused exclusively on the eyes-open condition in order to better preserve ocular dynamics within the extracted eye ICs. Consequently, the present findings cannot necessarily be generalized to eyes-closed EEG recordings. Furthermore, the dataset exhibited a moderate sex imbalance between the MDD and healthy control groups, which may have introduced potential demographic confounding effects. The medication status of the depressive subjects was also not available in the dataset and could therefore not be controlled for, despite the known influence of psychotropic treatments on electrophysiological and oculomotor activity.

Finally, ICA decomposition was performed using a 19-channel EEG montage, which may limit the stability and spatial specificity of source separation compared to higher-density EEG systems. Additional investigations on larger and more diverse datasets, combined with higher-density EEG acquisitions and external validation protocols, are necessary to more rigorously assess the physiological relevance and reproducibility of the reported findings.

Acknowledgements

The authors would like to acknowledge ***Wajid Mumtaz*** for making the dataset publicly available and facilitating its use in this study.

References

1. Castillo RJ, Guo KL. Implications of Dsm-5 for Health Care Organizations and Mental Health Policy. Journal of Health and Human Services Administration. 2016;39(2):217-244. https://doi.org/10.1177/107937391603900203
2. Hamilton M. A RATING SCALE FOR DEPRESSION. Journal of Neurology, Neurosurgery and Psychiatry. 1960;23(1):56-62. https://doi.org/10.1136/jnnp.23.1.56
3. BECK AT. An Inventory for Measuring Depression. Arch Gen Psychiatry. 1961;4(6):561. https://doi.org/10.1001/archpsyc.1961.01710120031004
4. Kaur C, Singh P, Sahni S. EEG Artifact Removal System for Depression Using a Hybrid Denoising Approach. BCN. 2021;12(4):465-476. https://doi.org/10.32598/bcn.2021.1388.2
5. Bee MA, Micheyl C. The cocktail party problem: What is it? How can it be solved? And why should animal behaviorists study it? Journal of Comparative Psychology. 2008;122(3):235-251. https://doi.org/10.1037/0735-7036.122.3.235
6. Movahed RA, Jahromi GP, Shahyad S, Meftahi GH. A major depressive disorder classification framework based on EEG signals using statistical, spectral, wavelet, functional connectivity, and nonlinear analysis. Journal of Neuroscience Methods. 2021;358:109209. https://doi.org/10.1016/j.jneumeth.2021.109209
7. Seifeddine B, Dib N. A Single-Channel EEG-Based Discrimination of Major Depressive Disorder with Wavelets Features and Machine Learning. 2023 International Conference on Networking and Advanced Systems (ICNAS). Published online October 21, 2023:1-6. https://doi.org/10.1109/icnas59892.2023.10330501
8. Saeedi A, Saeedi M, Maghsoudi A, Shalbaf A. Major depressive disorder diagnosis based on effective connectivity in EEG signals: a convolutional neural network and long short-term memory approach. Cogn Neurodyn. 2021;15(2):239-252. https://doi.org/10.1007/s11571-020-09619-0
9. Puthankattil SD, Joseph PK. Classification of EEG signals in normal and depression conditions by ANN using RWE and signal entropy. J Mech Med Biol. 2012;12(04):1240019. https://doi.org/10.1142/s0219519412400192
10. Baghernezhad S, Raouf P, Shalchyan V, Rostami R, Daliri MR. Graph theory analysis based on cross frequency coupling methods in major depressive disorder: A resting state EEG study. Computers in Biology and Medicine. 2025;198:111168. https://doi.org/10.1016/j.compbiomed.2025.111168
11. Bashir N, Narejo S, Naz B, et al. A Machine Learning Framework for Major Depressive Disorder (MDD) Detection Using Non-invasive EEG Signals. Wireless Pers Commun. 2023;140(1-2):39-61. https://doi.org/10.1007/s11277-023-10445-w
12. Sharma N, Sharma M, Tailor J, Chaudhari A, Joshi D, Acharya UR. Automated detection of depression using wavelet scattering networks. Med Eng Phys. 2024;124(1):104107. https://doi.org/10.1016/j.medengphy.2024.104107
13. Khandoker AH, Luthra V, Abouallaban Y, et al. Predicting depressed patients with suicidal ideation from ECG recordings. Med Biol Eng Comput. 2016;55(5):793-805. https://doi.org/10.1007/s11517-016-1557-y
14. Habib A, Vaniya SN, Khandoker A, Karmakar C. MDDBranchNet: A Deep Learning Model for Detecting Major Depressive Disorder Using ECG Signal. IEEE J Biomed Health Inform. 2024;28(7):3798-3809. https://doi.org/10.1109/jbhi.2024.3390847
15. Sharma N, Sharma M, Telangore H, Acharya UR. Automated accurate insomnia detection system using wavelet scattering method using ECG signals. Appl Intell. 2024;54(4):3464-3481. https://doi.org/10.1007/s10489-024-05284-6
16. Zitouni MS, Lih Oh S, Vicnesh J, Khandoker A, Acharya UR. Automated recognition of major depressive disorder from cardiovascular and respiratory physiological signals. Front Psychiatry. 2022;13. https://doi.org/10.3389/fpsyt.2022.970993
17. Henje Blom E, Olsson E, Serlachius E, Ericson M, Ingvar M. Heart rate variability (HRV) in adolescent females with anxiety disorders and major depressive disorder. Acta Paediatrica. 2010;99(4):604-611. https://doi.org/10.1111/j.1651-2227.2009.01657.x
18. Chen W, Zhong Q, Chen H, Chen S. Heart rate variability in children and adolescents with major depressive disorder: A systematic review and meta-analysis. Journal of Affective Disorders. 2023;335:204-215. https://doi.org/10.1016/j.jad.2023.05.022

19. Khandoker AH, Luthra V, Abouallaban Y, et al. Suicidal Ideation Is Associated with Altered Variability of Fingertip Photo-Plethysmogram Signal in Depressed Patients. Front Physiol. 2017;8. https://doi.org/10.3389/fphys.2017.00501
20. Ayoubipour S, Sho'ouri N. A Comparative Investigation of Wavelet Families for Classification of EOG Signals Related to Healthy and ADHD Children. Clin EEG Neurosci. 2023;55(1):11-21. https://doi.org/10.1177/15500594231192817
21. Banerjee A, Pal M, Datta S, Tibarewala DN, Konar A. Eye movement sequence analysis using electrooculogram to assist autistic children. Biomedical Signal Processing and Control. 2014;14:134-140. https://doi.org/10.1016/j.bspc.2014.07.010
22. Khushaba RN, Kodagoda S, Lal S, Dissanayake G. Driver Drowsiness Classification Using Fuzzy Wavelet-Packet-Based Feature-Extraction Algorithm. IEEE Trans Biomed Eng. 2011;58(1):121-131. https://doi.org/10.1109/tbme.2010.2077291
23. Piaseczna N, Duraj K, Doniec R, Tkacz E. Evaluation of Intoxication Level with EOG Analysis and Machine Learning: A Study on Driving Simulator*. 2023 45th Annual International Conference of the IEEE Engineering in Medicine and Biology Society (EMBC). Published online July 24, 2023:1-4. https://doi.org/10.1109/embc40787.2023.10340736
24. Wang L, Wang C, Li C, et al. AI-assisted multi-modal information for the screening of depression: a systematic review and meta-analysis. npj Digit Med. 2025;8(1). https://doi.org/10.1038/s41746-025-01933-3
25. Classifying major depression patients and healthy controls using EEG, eye tracking and galvanic skin response data - ClinicalKey. Accessed April 19, 2026. https://www.clinicalkey.com/#!/content/playContent/1-s2.0-S0165032718330064?returnurl=null&referrer=null
26. Zhu F, Zhang J, Dang R, Hu B, Wang Q. MTNet: Multimodal transformer network for mild depression detection through fusion of EEG and eye tracking. Biomedical Signal Processing and Control. 2025;100:106996. https://doi.org/10.1016/j.bspc.2024.106996
27. Shen R, Zhan Q, Wang Y, Ma H. Depression Detection by Analysing Eye Movements on Emotional Images. ICASSP 2021 - 2021 IEEE International Conference on Acoustics, Speech and Signal Processing (ICASSP). Published online June 6, 2021:7973-7977. https://doi.org/10.1109/icassp39728.2021.9414663
28. Carney RM, Hong BA, Kulkarni S, Kapila A. A comparison of EMG and SCL in normal and depressed subjects. Pav J Biol Sci. 1981;16(4):212-216. https://doi.org/10.1007/bf03003361
29. Greden JF. Facial Electromyography in Depression. Arch Gen Psychiatry. 1986;43(3):269. https://doi.org/10.1001/archpsyc.1986.01800030087009
30. Carney RM, Hong BA, O'Connell MF, Amado H. Facial Electromyography as a Predictor of Treatment Outcome in Depression. Br J Psychiatry. 1981;138(6):485-489. https://doi.org/10.1192/bjp.138.6.485
31. Greden JF, Price HL, Genero N, Feinberg M, Levine S. Facial EMG activity levels predict treatment outcome in depression. Psychiatry Research. 1984;13(4):345-352. https://doi.org/10.1016/0165-1781(84)90082-9
32. A. Ramadan M, Salem NM, Mahmoud LN, Sadek I. Multimodal machine learning approach for emotion recognition using physiological signals. Biomedical Signal Processing and Control. 2024;96:106553. https://doi.org/10.1016/j.bspc.2024.106553
33. Kose MR, Ahirwal MK, Kumar A. A new approach for emotions recognition through EOG and EMG signals. SIViP. 2021;15(8):1863-1871. https://doi.org/10.1007/s11760-021-01942-1
34. Kelati A, Plosila J, Tenhunen H. Machine Learning for sEMG Facial Feature Characterization. 2019 Signal Processing: Algorithms, Architectures, Arrangements, and Applications (SPA). Published online September 2019:169-174. https://doi.org/10.23919/spa.2019.8936818
35. Barigala VK, Sriram Kumar P, Govarthan PK, et al. Identifying the Optimal Location of Facial EMG for Emotion Detection Using Logistic Regression. Studies in Health Technology and Informatics. Published online June 29, 2023. https://doi.org/10.3233/shti230429
36. Kołodziej M, Majkowski A, Jurczak M. Acquisition and Analysis of Facial Electromyographic Signals for Emotion Recognition. Sensors. 2024;24(15):4785. https://doi.org/10.3390/s24154785
37. Cai Y, Guo Y, Jiang H, Huang MC. Machine-learning approaches for recognizing muscle activities involved in facial expressions captured by multi-channels surface electromyogram. Smart Health. 2018;5-6:15-25. https://doi.org/10.1016/j.smhl.2017.11.002
38. Kehri V, Ingle R, Patil S, Awale RN. Analysis of Facial EMG Signal for Emotion Recognition Using Wavelet Packet Transform and SVM. Advances in Intelligent Systems and Computing. Published online August 8, 2018:247-257. https://doi.org/10.1007/978-981-13-0923-6_21
39. Schwartz GE, Fair PL, Salt P, Mandel MR, Klerman GL. Facial Expression and Imagery in Depression: An Electromyographic Study. Psychosomatic Medicine. 1976;38(5):337-347. https://doi.org/10.1097/00006842-197609000-00006
40. Greden JF. Facial Electromyography in Depression. Arch Gen Psychiatry. 1986;43(3):269. https://doi.org/10.1001/archpsyc.1986.01800030087009
41. Carney RM, Hong BA, O'Connell MF, Amado H. Facial Electromyography as a Predictor of Treatment Outcome in Depression. Br J Psychiatry. 1981;138(6):485-489. https://doi.org/10.1192/bjp.138.6.485
42. Mumtaz W, Xia L, Ali SSA, Yasin MAM, Hussain M, Malik AS. Electroencephalogram (EEG)-based computer-aided technique to diagnose major depressive disorder (MDD). Biomedical Signal Processing and Control. 2017;31:108-115. https://doi.org/10.1016/j.bspc.2016.07.006
43. Mallat S. Group Invariant Scattering. Comm Pure Appl Math. 2012;65(10):1331-1398. https://doi.org/10.1002/cpa.21413
44. Yu Y, Si X, Hu C, Zhang J. A Review of Recurrent Neural Networks: LSTM Cells and Network Architectures. Neural Computation. 2019;31(7):1235-1270. https://doi.org/10.1162/neco_a_01199
45. Delorme A, Makeig S. EEGLAB: an open source toolbox for analysis of single-trial EEG dynamics including independent component analysis. Journal of Neuroscience Methods. 2004;134(1):9-21. https://doi.org/10.1016/j.jneumeth.2003.10.009
46. Lee TW, Girolami M, Sejnowski TJ. Independent Component Analysis Using an Extended Infomax Algorithm for Mixed Subgaussian and Supergaussian Sources. Neural Computation. 1999;11(2):417-441. https://doi.org/10.1162/089976699300016719
47. Bell AJ, Sejnowski TJ. An Information-Maximization Approach to Blind Separation and Blind Deconvolution. Neural Computation. 1995;7(6):1129-1159. https://doi.org/10.1162/neco.1995.7.6.1129
48. Pion-Tonachini L, Kreutz-Delgado K, Makeig S. The ICLabel dataset of electroencephalographic (EEG) independent component (IC) features. Data in Brief. 2019;25:104101. https://doi.org/10.1016/j.dib.2019.104101
49. Buriro AB, Ahmed B, Baloch G, et al. Classification of alcoholic EEG signals using wavelet scattering transform-based features. Computers in Biology and Medicine. 2021;139:104969. https://doi.org/10.1016/j.compbiomed.2021.104969
50. Barmpas K, Panagakis Y, Adamos DA, Laskaris N, Zafeiriou S. BrainWave-Scattering Net: a lightweight network for EEG-based motor imagery recognition. J Neural Eng. 2023;20(5):056014. https://doi.org/10.1088/1741-2552/acf78a
51. Jiang X, Bian GB, Tian Z. Removal of Artifacts from EEG Signals: A Review. Sensors. 2019;19(5):987. https://doi.org/10.3390/s19050987
52. Carvalho N, Laurent E, Noiret N, et al. Eye Movement in Unipolar and Bipolar Depression: A Systematic Review of the Literature. Front Psychol. 2015;6. https://doi.org/10.3389/fpsyg.2015.01809
53. Jergelova M, Jagla F. Central and peripheral correlates of eye movements in selected mood disorders. Neuro Endocrinol Lett. 2010;31(6):731-737.

54. Cruz A, Garcia D, Pires G, Nunes U. Facial Expression Recognition based on EOG toward Emotion Detection for Human-Robot Interaction. In: 2025:31-37. Accessed November 30, 2025. https://www.scitepress.org/PublicationsDetail.aspx?ID=TTrByNwiHfY=&t=1

55. Thier P. The Oculomotor Cerebellum. Oxford University Press; 2011. https://doi.org/10.1093/oxfordhb/9780199539789.013.0010

56. Lynch JC, Tian JR. Cortico-cortical networks and cortico-subcortical loops for the higher control of eye movements. Progress in Brain Research. Published online 2006:461-501. https://doi.org/10.1016/s0079-6123(05)51015-x

57. Pouget P. The cortex is in overall control of 'voluntary' eye movement. Eye. 2014;29(2):241-245. https://doi.org/10.1038/eye.2014.284

58. McMenamin BW, Shackman AJ, Greischar LL, Davidson RJ. Electromyogenic artifacts and electroencephalographic inferences revisited. NeuroImage. 2011;54(1):4-9. https://doi.org/10.1016/j.neuroimage.2010.07.057

59. Korb S, Grandjean D, Scherer K. Investigating the production of emotional facial expressions: a combined electroencephalographic (EEG) and electromyographic (EMG) approach. 2008 8th IEEE International Conference on Automatic Face and Gesture Recognition. Published online September 2008:1-6. https://doi.org/10.1109/afgr.2008.4813388

60. Künecke J, Hildebrandt A, Recio G, Sommer W, Wilhelm O. Facial EMG Responses to Emotional Expressions Are Related to Emotion Perception Ability. Gray M, ed. PLoS ONE. 2014;9(1):e84053. https://doi.org/10.1371/journal.pone.0084053

61. RIHS T, MICHEL C, THUT G. A bias for posterior α-band power suppression versus enhancement during shifting versus maintenance of spatial attention. NeuroImage. 2009;44(1):190-199. https://doi.org/10.1016/j.neuroimage.2008.08.022

62. Helfrich RF, Huang M, Wilson G, Knight RT. Prefrontal cortex modulates posterior alpha oscillations during top-down guided visual perception. Proc Natl Acad Sci USA. 2017;114(35):9457-9462. https://doi.org/10.1073/pnas.1705965114

63. Banerjee S, Snyder AC, Molholm S, Foxe JJ. Oscillatory Alpha-Band Mechanisms and the Deployment of Spatial Attention to Anticipated Auditory and Visual Target Locations: Supramodal or Sensory-Specific Control Mechanisms? Journal of Neuroscience. 2011;31(27):9923-9932. https://doi.org/10.1523/jneurosci.4660-10.2011

64. Jiang H, Popov T, Jylänki P, et al. Predictability of depression severity based on posterior alpha oscillations. Clinical Neurophysiology. 2016;127(4):2108-2114. https://doi.org/10.1016/j.clinph.2015.12.018

65. Umemoto A, Panier LYX, Cole SL, Kayser J, Pizzagalli DA, Auerbach RP. Resting posterior alpha power and adolescent major depressive disorder. Journal of Psychiatric Research. 2021;141:233-240. https://doi.org/10.1016/j.jpsychires.2021.07.003

66. Delorme A. EEG is better left alone. Sci Rep. 2023;13(1). https://doi.org/10.1038/s41598-023-27528-0